Effect of Size of Man-Made and Natural Mineral Fibers on Chemiluminescent Response in Human Monocyte-Derived Macrophages

Masayuki Ohyama,[1] Toru Otake,[1] and Kenji Morinaga[2]

[1]Osaka Prefectural Institute of Public Health, Nakamichi, Higashinari-ku, Osaka, Japan; [2]Osaka Medical Center for Cancer and Cardiovascular Diseases, Nakamichi, Higashinari-ku, Osaka, Japan

Fiber size is an important factor in the tumorigenicity of various mineral fibers and asbestos fibers in animal experiments. We examined the time course of the ability to induce lucigenin-dependent chemiluminescence (CL) from human monocyte-derived macrophages exposed to Japan Fibrous Material standard reference samples (glass wool, rock wool, micro glass fiber, two types of refractory ceramic fiber, refractory mullite fiber, potassium titanium whisker, silicon carbide whisker, titanium oxide whisker, and wollastonite). We determined how fiber length or width might modify the response of cells. We found that the patterns of time-dependent increase of CL (sigmoid type) were similar for each sample except wollastonite. We observed a strong correlation between geometric-mean length and ability to induce CL in seven samples > 6 μm in length over the time course (largest r^2 = 0.9760). Although we also observed a close positive correlation between geometric-mean width and the ability to induce CL in eight samples < 1.8 μm in width at 15 min (r^2 = 0.8760), a sample of 2.4 μm in width had a low ability to induce CL. Moreover, the relationship between width and the rate of increase in ability to induce CL had a negative correlation at 30–60 min (largest r^2 = 0.7473). Our findings suggest that the release of superoxide from macrophages occurs nonspecifically for various types of mineral fibers depending on fiber length.

***Key words*: fiber length, glass wool, macrophage, man-made mineral fibers, micro glass fiber, reactive oxygen species, refractory ceramic fiber, rock wool, silicon carbide whisker, superoxide.**
***Environ Health Perspect* 109:1033–1038 (2001). [Online 27 September 2001]**
http://ehpnet1.niehs.nih.gov/docs/2001/109p1033-1038ohyama/abstract.html

Exposure to amphibole asbestos is associated with the development of mesotheliomas, lung cancers, and fibrotic lung diseases (*1,2*). Therefore, man-made and natural mineral fibers often have been substituted for asbestos. Although numerous inhalation studies demonstrated no significant increase in tumor incidence in animals exposed to such substitutes (*3–5*), several mineral fibers (refractory ceramic fiber and fiber glass) were carcinogenic in rodent chronic inhalation studies (*6,7*). Morover, in animal intraperitoneal studies, the fiber length of asbestos and other mineral fibers has been found to be one of the major descriptors of tumorigenicity (*8–10*). Therefore, we considered that the extensive knowledge on asbestos may apply to other mineral fibers' tumorigenicity.

The concept that reactive oxygen species (ROS) such as hydrogen peroxide, superoxide, and the hydroxyl radical may underlie the pathogenesis of derangement has become the focus of extensive research in asbestos fibers (*11*). Reactive oxygen species, especially the hydroxyl radical, can alter biologic macromolecules including proteins, cell membrane lipids, DNA, and RNA, causing cellular dysfunction, cytotoxicity, and possibly malignant transformation from asbestos fibers (*11–13*).

However, hydroxyl radical activity differs among three tumorigenic fibers: amosite asbestos, silicon carbide, and refractory ceramic fiber (RCF). Amosite and RCF release hydroxyl radicals, whereas silicon carbide fibers have no hydroxyl radical activity (*13*). Therefore, although hydroxyl radical activity may increase the tumorigenicity of mineral fibers it is not necessary for it to occur. Moreover, the results from numerous intrapleural studies led to the conclusion that basically all types of elongated dust particles can induce tumors if they are sufficiently long, thin, and durable in the tissue (*5,8,10,15*). Our study focuses on the superoxide induced in asbestos or other mineral fibers, and on the relationship between the ability to induce superoxide and the fiber size of various mineral fibers.

Long asbestos fibers, such as chrysotile and amosite, are more effective than short fibers in eliciting the release of superoxide from macrophages (*16*). Among various mineral particles, fibrous dust causes a significant increase in the release of superoxide from macrophages (*11,17*), whereas nonfibrous particles were less active in this regard (*18*). However, only a few studies have examined in detail the relationship between length and release of superoxide with man-made mineral fibers (*19,20*). Moreover, it was suggested that fiber length is not an important factor in the ability of man-made mineral fibers to induce production of reactive oxygen species in polymorphonuclear leukocytes (*19*).

We demonstrated previously a method for comparing the ability to induce lucigenin-dependent chemiluminescence (CL) per fiber from human monocyte-derived macrophages exposed to nine types of mineral fibers of different sizes at the acute phase of the response (*20*). We observed that the ability to induce CL increased with fiber length at the acute phase of the response, when the mineral fibers were longer than approximately 6 μm. Our purpose in this study was to investigate the time course of the relationship between fiber length and the ability to induce CL, and to determine how fiber width might modify this response with various mineral fibers.

Materials and Methods

Mineral fibers. We used the Japan Fibrous Material (JFM) standard reference samples provided by the Japan Fibrous Material Research Association (*21*), designated by geometric-mean length (micrometers), geometric-mean width (micrometers), and number of fibers per unit weight (micrograms): glass wool (GW1, 20.0 μm; 0.88 μm; 0.7 × 10^3/μg); rock wool (RW1, 16.5, 1.8, 1.7); micro glass fiber (MG1, 3.0, 0.24, 65); refractory ceramic fiber (RF1, 12.0, 0.77, 8.8; RF2, 11.0, 1.1, 8.7); refractory mullite fiber (RF3, 11.0, 2.4, 3.5); potassium titanium whisker (PT1, 6.0, 0.35, 590); silicon carbide whisker (SC1, 6.4, 0.30, 410); titanium oxide whisker (TO1, 2.1, 1.00, 640); and wollastonite (WO1, 10.5, 1.00, 24). The characterization of these fibers has been documented elsewhere (*21,22*). For example, chemical composition of these fibers has been demonstrated by X-ray fluorescence analysis. Fe_2O_3 is the only iron compound which was detected in all samples (chemical composition of Fe_2O_3, by percentage: GW1, 0.28; RW1, 0.41; MG1, 0.07; RF1, 0.15; RF2, 0.04; RF3, 0.05; PT1, 0.02; SC1, 0.07; TO1, 0.04; and WO1, 0.30). Each sample was dried and heat-sterilized at 80°C for 48 hr and suspended in fetal bovine serum (FBS) at a concentration of 1 mg/mL. The suspensions were incubated for 15 min at 37°C, and spin-washed three times in Hanks' balanced

Address correspondence to M. Ohyama, Osaka Prefectural Institute of Public Health, 1-3-69, Nakamichi, Higashinari-ku, Osaka 537-0025, Japan. Telephone: +81-6-6972-1321 Fax: +81-6-6972-2393. E-mail: ooyama@iph.pref.osaka.jp

We thank the Japan Fibrous Material Research Association for supplying the Japan Fibrous Material standard reference samples.

Received 25 December 2000; accepted 4 April 2001.

salt solution (HBSS), at 900*g* for 20 min. Pellets were resuspended at stepped suspension concentrations from 10/13 mg/mL to 10 mg/mL, except SC1, which was adjusted to one-tenth the concentration of other samples. These suspensions were stored at 4°C.

Cell isolation. We obtained heparinized blood from healthy donors by venipuncture and diluted it 1:1 in HBSS. We isolated monocyte–lymphocyte fractions by Ficoll density centrifugation and plated them in 9-cm-diameter plastic tissue culture dishes for monocyte adherence (*23*). We cultured the adhering cells for 9 days in RPMI1640 HEPES modification (Sigma Chemical Co., St. Louis, MO, USA) with 10% FBS, 100 U/mL penicillin, and 100 µg/mL streptomycin. This culture medium was changed every 2 days. Adherent cells were separated after 6 days, and suspended in serum-free RPMI1640.

Chemiluminescence measurements. The method of measurement of lucigenin-dependent CL from 6-day-old human monocyte-derived macrophages exposed to various mineral fibers has been described (*24*): The lucigenin responses increased with the increasing age of cultures over 6 days, and Nyberg and Klockars (*24*) obtained a correlation between lucigenin-dependent CL and superoxide production measured with the cytochrome C reduction assay at 6 days of culture.

The isolated cells (1×10^5 cells) were transferred into a luminometer tube containing mineral sample suspension (65 µL), 10% FBS, 0.1 mM lucigenin, and in some experiments 1,000 U/mL superoxide dismutase (SOD). The final volume of each tube was 1 mL. The light emission of each sample was detected at 15-min intervals with a luminescence reader (ALOKA BLR-201; Mitaka, Tokyo, Japan). We measured all samples including the negative control (no fiber) with the same cell suspension at 10-sec intervals. We performed all reactions at 37°C in RPMI 1640, each measurement 4 times.

Statistical analysis. We analyzed the ability to induce CL per fiber of each sample as described previously (*20*). Briefly, we examined the relation between the estimated number of fibers administered and CL response by linear regression. The slope (β_1) of the regression line was taken as a measure of the ability to induce CL per fiber. We excluded the data of β_1 for $r^2 < 0.9$. We also examined the relation between fiber size and ability to induce CL by linear regression, and calculated the increase in the rate of induction with two β_1. We examined the time course of the increase in the ability to induce CL by power regression. Finally, we examined the relation between fiber size and increased ability to induce CL using linear regression.

Results

The time course of the ability to induce CL per fiber (β_1). We tested the CL response of all JFM preparations and controls at constant rotation every 15 min by using a stock of cells in suspension. We needed β_1 to compare the CL response of each sample at a value not related to the number of fibers administered. Table 1 shows β_1 and r^2. All fiber samples except for WO1 induced a CL response in a dose-dependent manner. Each response was almost completely inhibited by SOD, which is a superoxide scavenger (data not shown). WO1 was excluded in subsequent analyses because its CL response increased rectilinearly and the linearity of its dose response was low (Table 1). Moreover, we also excluded the β_1 data for $r^2 < 0.9$ at each measurement time.

As shown in Figure 1, each JFM standard reference sample produced a sigmoid-type increase in β_1. The pattern of increase in β_1 for each sample was similar, although the values differed.

The similarity of the increase in β_1 to JFM samples. We calculated the rate of increase in β_1 to demonstrate the similarity of the response pattern to various mineral fibers. Table 2 shows the rate for each time point. Although each rate of increase was different at 15–30, the kinetics of the rate were relatively similar in these cases. As shown in Figure 2, the rate of β_1 decreased for the power regression line. Table 3 shows constants and the r^2 of the power regression lines. These comparisons showed the similarity of each CL response more clearly. However, the thickest fiber (RF3) and the thinnest fiber (TO1) had slightly lower correlations than other samples. The rate of RF3 was low in the acute phase, and the rate of TO1 was high in the acute phase.

The relationship between β_1 and fiber length. Figure 3 shows a representative time-dependent relation between geometric-mean length and β_1, used to examine the effect of fiber length on CL response. The results are shown in Table 4 with constants and the r^2 of the regression lines. A close correlation existed between length and β_1 at each time point, although four samples under approximately 6 µm in length (SC1, PT1, MG1, and TO1) had a low β_1. Therefore, a further close correlation existed between length and β_1 with samples > 6 µm in length (GW1, RW1, RF1, RF2, RF3, SC1, and PT1) after

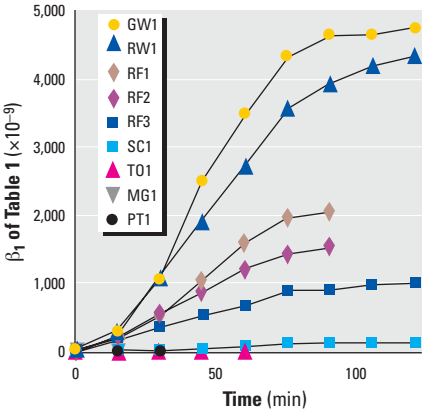

Figure 1. Time course of ability to induce CL from macrophages exposed to various mineral fibers (β_1 of Table 1). Each point is the mean from four measurements. The defects are the cases where r^2 is < 0.9 (shown in Table 1).

Table 1. Constants and r^2 of the regression lines for CL and estimated number of fibers.

Time[a]	0		15		30		45		60		75		90		105		120	
(min)	β_1[b]	r^2[c]	β_1	r^2	β_1	r^2	β_1	r^2	β_1	r^2	β_1	r^2	β_1	r^2	β_1	r^2	β_1	r^2
GW1	15.34	0.110	280.0	0.960	1,052	0.958	2,492	0.942	3,489	0.927	4,333	0.941	4,643	0.920	4,642	0.947	4,735	0.940
RW1	9.869	0.406	345.4	0.966	1,072	0.979	1,920	0.961	2,735	0.959	3,581	0.952	3,946	0.924	4,209	0.937	4,352	0.938
MG1	0.436	0.339	21.97	0.972	66.20	0.902	112.1	0.818	153.8	0.815	182.0	0.819	179.8	0.798	162.7	0.761	142.2	0.735
RF1	0.664	0.020	168.3	0.920	517.9	0.992	1,021	0.985	1,601	0.975	1,955	0.952	2,035	0.928	1,877	0.865	1,580	0.780
RF2	–0.75	0.028	214.3	0.985	562.2	0.988	893.9	0.967	1,219	0.944	1,447	0.921	1,538	0.916	1,439	0.897	1,327	0.848
RF3	7.742	0.422	177.0	0.978	371.0	0.992	539.1	0.979	669.1	0.937	910.5	0.982	914.7	0.970	997.0	0.970	1,021	0.967
PT1	–0.03	0.162	2.130	0.971	6.100	0.940	9.600	0.896	11.40	0.818	10.40	0.685	8.900	0.608	6.700	0.484	4.800	0.373
SC1	0.307	0.228	7.600	0.917	24.40	0.992	49.20	1.000	77.80	0.996	110.6	0.996	123.1	0.994	128.9	0.992	132.4	0.990
TO1	–0.03	0.203	1.520	0.977	3.200	0.974	7.000	0.988	11.00	0.913	12.00	0.822	11.10	0.738	9.400	0.662	7.300	0.607
WO1	–0.29	0.072	–5.69	0.450	–2.90	0.041	8.900	0.124	28.20	0.338	61.80	0.580	95.30	0.688	118.8	0.765	137.1	0.786

[a]Time after administration; CL responses of 54 samples were measured in constant rotation at 15–min intervals with the same stock suspension of cells. [b]β_1 ($\times 10^{-9}$) is the slope of the regression line for the estimated number of fibers administered and CL response with 5 concentrations and a duplicate negative control. The CL response is the mean value of the four measurements. [c]Square of the correlation coefficient of the regression line.

30 min. The relation between length and β_1 lasted from the acute phase of the reaction to 120 min.

The relationship between β_1 and fiber width. The World Health Organization (WHO) classifies mineral fibers based on length, width, and the aspect ratio of the fiber (*25*). Figure 4 shows the relation between geometric-mean width and β_1 at 15 and 45 min. The results are shown in Table 5 with constants and the r^2 of the regression lines. As shown in Figure 4 and Table 5, we observed a close correlation between width and β_1 for eight samples < 1.8 μm in width at 15 min (r^2 = 0.8766); however, this relationship did not continue (r^2 at 45 min = 0.5138). β_1 correlated with width more than with length at 15 min, but it correlated with length more than with width after 30 min.

The relationship between increase rate of β_1 and width. We examined the relationship between rate of β_1 and fiber width to demonstrate the effect of the width from 15 to 60 min. Figure 5 shows a representative relationship between rate of β_1 and fiber width. The results are shown in Table 6 with constants and the r^2 of the regression lines. Although the tendency of this relationship at 15–30 min resembles that of β_1 and width at 15 min (Figure 4A), we observed a correlation at 30–45 min [r^2 = 0.5309 (Figure 5B)] and at 45–60 min [r^2 = 0.7473 (Figure 5C)]. However, a slope of the regression line decreased over the time course. Moreover, as shown in Table 2, the increase of β_1 was similar in each sample after 60 min. Therefore, we saw no correlation at 60–75 min (Table 6).

The relationship between increase rate of β_1 and length. We also examined the relation between rate of β_1 and fiber length. The correlation between these could not be recognized at any time point (data not shown).

The relationship between CL response and fiber sample weight. The relationship between sample weight and CL response at 45 min is shown in Figure 6A. These data were the most rectilinear for the dose–response curve in the time-course measurement. Table 7 shows a slope of regression line of the dose–response curves in mass concentration. MG1 had the highest level, and GW1 and RF3 had the lowest level. However, the linearity of dose–response curves did not continue in some samples. The relationship between sample weight and CL response at 120 min is shown in Figure 6B as reference. The dose–response curve of some samples was saturated at various levels. Short fibers tend to saturate the dose–response curve at low dosage.

Table 2. Time course of the rate of increase in β_1, in 15-min intervals.

No.[a]	1 (15–30)	2 (30–45)	3 (45–60)	4 (60–75)	5 (75–90)	6 (90–105)	7 (105–120)
GW1	3.757	2.369	1.400	1.242	1.072	1.000	1.020
RW1	3.104	1.791	1.424	1.309	1.102	1.067	1.034
MG1	3.012	—[b]	—	—	—	—	—
RF1	3.078	1.971	1.569	1.221	1.041	—	—
RF2	2.623	1.590	1.364	1.186	1.063	—	—
RF3	2.096	1.453	1.241	1.361	1.005	1.090	1.024
PT1	2.845	—	—	—	—	—	—
SC1	3.216	2.013	1.582	1.421	1.113	1.047	1.027
TO1	2.131	2.165	1.572	—	—	—	—
Average	2.874	1.907	1.450	1.290	1.066	1.051	1.026
SD	0.498	0.296	0.120	0.082	0.036	0.033	0.005

[a]Time-course order of the rate of increase in β_1. The rates were calculated between continuing two data points, in minutes. For example, the values at 1 are β_1 at 30 min divided by the β_1 at 15 min. [b]The defects were the cases where r^2 < 0.9.

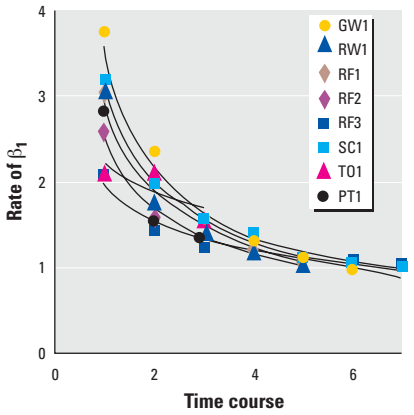

Figure 2. Time course of the increase in β_1. The defects are the cases where r^2 is < 0.9. The curves were approximated by power regression.

Table 3. Constants and the r^2 of the power regression lines for time course of the rate of increase in β_1.

Fibers	A[a]	B[a]	r^{2b}	n^c
GW1	3.601	–0.720	0.961	7
RW1	2.849	–0.563	0.970	7
MG1	–	–	–	1
RF1	3.123	–0.669	0.9959	5
RF2	2.512	–0.550	0.9829	5
RF3	1.983	–0.356	0.8972	7
PT1	–	–	–	1
SC1	3.136	–0.693	0.9889	7
TO1	2.240	–0.245	0.5681	3

[a]Constants of the power regression line for the time course of the rate in Figure 2. For convenience, numbering was used to estimate the regression line. Equation, $Y = AX^B$; Y = rate of increase in Table 2, X = numbering of the rate in Table 2. [b]Square of the correlation coefficient of the power regression line. Though constant, A changes with the numbering; constant B and r^2 are fixed. [c]Effective number.

Discussion

The results of the present study demonstrate the time course and rate of the induction of lucigenin-dependent CL in human monocyte-derived macrophages for various man-made and natural mineral fibers. Moreover, we examined the time-dependent relationships between fiber size and these parameters. Even when the dosed number of fibers differed for each sample, the ability to induce CL per fiber could be approximated using our analysis.

Many intrapleural studies led to the conclusion that the fibrous shape of asbestos dust particles is the cause of their carcinogenicity in humans and that basically all types of elongated dust particles such as mineral and vitreous fibers can induce tumors if they are sufficiently long, thin, and durable in the tissue (*10,26*). If this conclusion is true, common reactivity in the mechanism of tumor induction should exist between asbestos and mineral and vitreous fibers. Numerous studies have suggested that ROS may underlie the pathogenesis of asbestos-related lung diseases (*11,27*). However, amphibole asbestos, which includes iron in its fibers, plays a special role in ROS-mediated pathology because it catalyzes the generation of the reactive hydroxyl radical from hydrogen peroxide (*11,28,29*). In asbestos, the hydroxyl radical can alter various biologic effects (*11–13*). In biologic systems, superoxide usually acts as the reductant producing Fe^{2+}, which rapidly decomposes hydrogen peroxide to hydroxyl radicals (*29,30*). The action of superoxide makes a chain of reactions in which the net process converts hydrogen peroxide to the hydroxyl radical (*29,31*). Paradoxically, superoxide activity may decide hydroxyl radical activity *in vivo*, because hydrogen peroxide has always been made *in vivo* if Fe^{3+} exists in close proximity. Various mineral fibers cause a significant increase in the release of superoxide from macrophages (*18,19*). Moreover, tumorigenic fibers do not always have hydroxyl radical activity *in vitro* (*14*). Silicon carbide fibers, one type of tumorigenic fiber, have no hydroxyl radical activity (*14*). Our findings here suggest that macrophages have common superoxide reactivity for various types of fiber and that the activity of superoxide from macrophages has an important role in biologic effects, depending on fiber length.

In early animal intraperitoneal studies, it was suggested that the induction of pleural sarcoma increased with the length of fibers with diameters < 1.5 μm (*32*). However, a

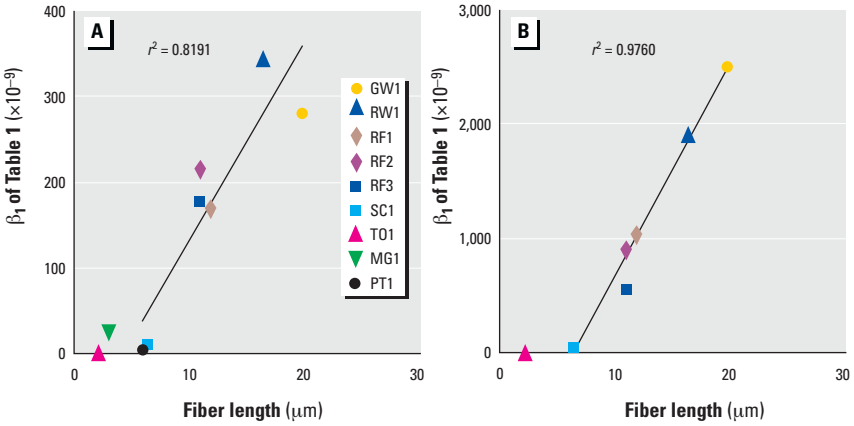

Figure 3. The relationship between geometric-mean length and β_1 of Table 1. The line is a regression line for samples > 6 μm in length. The data for r^2 < 0.9 were excluded. (*A*) Data at 15 min; this correlation is the lowest. (*B*) Data at 45 min; this correlation is the highest.

Table 4. Constants and the r^2 of the regression lines for β_1 of Table 1 and fiber length.

Time[a]	0	15	30	45	60	75	90	105	120
A[b]	0.080	2.027	68.27	149.7	211.2	332.1	360.7	367.3	376.2
B[b]	–4.062	–6.286	–259.1	–700.4	–983.5	–2,200	–2,423	–2,456	–2,509
r^{2c}	0.677	0.852	0.906	0.916	0.907	0.965	0.957	0.946	0.943
n^d	9	9	9	7	7	6	6	4	4
A[e]	1.068	23.04	82.77	186.8	263.2	332.1	360.7	367.3	376.2
B[e]	–7.910	–102.2	–465.1	–1,241	–1,741	–2,200	–2,423	–2,456	–2,509
r^{2f}	0.738	0.819	0.937	0.976	0.962	0.965	0.957	0.946	0.943
n	7	7	7	6	6	6	6	4	4

[a]Time after administration (min). [b]Analysis for nine samples. A and B are constants of the regression line for β_1 and fiber length. Equation: Y = AX + B; Y = β_1 of Table 1, X = geometric-mean length of fibers, A, B = constants (× 10^{-9}). [c]Square of the correlation coefficient of the regression line with whole samples. [d]Effective number. The data < 0.9 in r^2 of Table 1 were excluded, except for time 0. The data of time 0 are reference data. All effective data after 75 min were samples > 6 μm in length. [e]Analysis for seven samples > 6 μm in length. A,B and equation were the same as *b*. [f]Square of the correlation coefficient of the regression line with samples > 6 μm in length.

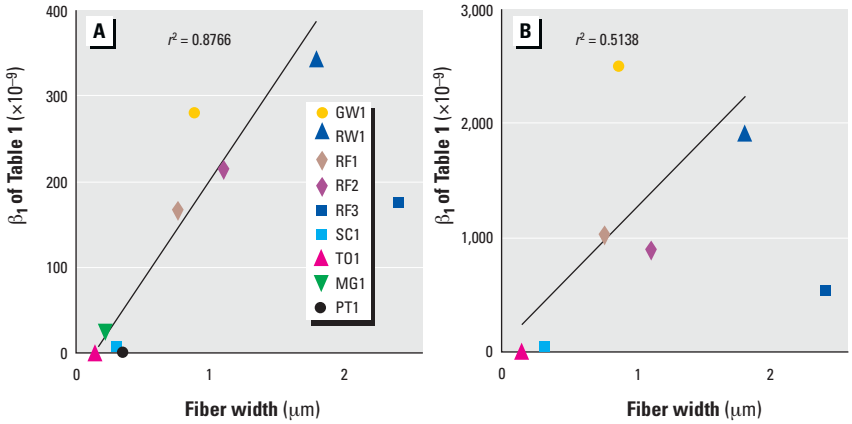

Figure 4. The relationship between geometric-mean width and β_1 of Table 1. The continuous line is a regression line with samples < 1.8 μm in width. (*A*) Data at 15 min; this correlation is the highest. (*B*) Data at 45 min.

Table 5. Constants and the r^2 of the regression lines for β_1 of Table 1 and fiber width, except RF3.

Time[a]	0	15	30	45	60	75	90	105	120
A[b]	5.930	232.8	719.7	1,196	1,686	1,917	2,134	2,429	2,519
B[b]	-0.911	-32.26	-88.98	68.85	119.7	426.2	386.6	580.1	571.3
r^{2c}	0.311	0.877	0.775	0.514	0.515	0.387	0.407	0.545	0.556
n^d	8	8	8	6	6	5	5	3	3

[a]Time after administration (min). [b]Analysis for eight samples < 1.8 μm in width. A and B are constants of the regression line for β_1 and fiber width. Equation: Y = AX+B; Y = β_1 of Table 1, X = geometric-mean width of fibers, A,B = constants (× 10^{-9}). [c]Square of the correlation coefficient of the regression line. [d]Effective number. The data < 0.9 in r^2 of Table 1 were excluded, except for time 0. The data of time 0 are reference data.

relation between ROS and fiber width has not been shown. We also tried to analyze the effect of fiber width on the ability to induce CL. Our results showed that wide fiber (a width of 2.4 μm) has a low ability to induce CL and that thin fibers cause a large acceleration in the induction of CL in the acute phase. However, our findings suggest that the superoxide-mediated biologic effect of width is weak because the effect of width on the ability to induce CL was smaller than that of length. If a biologic effect of width does exist, thin fibers may be stronger than thick fibers of the same length.

WHO has classified fibers > 5 μm long, < 3 μm diameter, with an aspect ratio > 3:1 (*25*). Our findings suggest that many airborne WHO fibers induce superoxide release from macrophages depending on fiber length.

Long asbestos fibers are more effective than short fibers in eliciting the release of superoxide from macrophages (*16*). However, the molecular mechanism by which asbestos may augment the release of oxygen metabolites from phagocytic cells is unclear. One hypothesis is that oxidant release occurs nonspecifically during "frustrated" phagocytosis by alveolar macrophages and polymorphonuclear leukocytes that are unable to ingest long asbestos fibers completely (*33*). However, our findings do not support this hypothesis, because the time-dependent pattern (sigmoid type) and increase of ability to induce CL were similar for each sample except wollastonite (Figures 1,2). These findings suggest that though the release of superoxide from macrophages occurs nonspecifically for many mineral fibers, the intensity had already been decided when fibers were phagocytosed to some extent. If the release of superoxide occurs during "frustrated" phagocytosis, the intensity of that of short fibers should decrease with the advance of phagocytosis.

We speculated as to the reason why the ability to induce CL increased with fiber length when samples were longer than approximately 6 μm. The regular transition in the rate to induce CL in each sample suggests that the intensity of the CL response is decided at the initial stage of phagocytosis. However, it cannot be considered that macrophages recognized fiber length at the initial stage of phagocytosis. In observations

by optical microscope, short fibers were perpendicularly phagocytosed, and long fibers were often tangentially phagocytosed (data not shown). Therefore, we speculated that tangential phagocytosis has a stronger effect on the ability to induce CL than perpendicular phagocytosis. If this speculation is true, a cause of the enhanced ability to induce CL may be the increase in the tangential phagocytic rate with lengthening of fiber. Moreover, we speculated that tangential phagocytosis shifts to perpendicular phagocytosis with fibers under approximately 6 μm in length.

In general, many experimental protocols have been conducted based on the mass concentration of fiber samples. Therefore, we also show the CL response per sample weight (Figure 6A) to allow comparison with other experimental results. In comparison by mass concentration, our data showed that the CL response is weak in both the short samples and samples such as glass wool and rock wool, which have low fiber numbers per unit weight. Mass concentration study of glass wool and rock wool showed no significant increase in tumor incidence in rats (*4,5*). The data in Figure 6A are consistent with these *in vivo* results. Moreover, a durable special application fiber glass (MMVF33, 106 fibers/cc > 20 μm) induced lung fibrosis and a single mesothelioma in hamsters; however, insulation fiber glass (MMVF10a, 151 fibers/cc > 20 μm) did not induce lung fibrosis or tumors (*34*). The data in Figure 1 are consistent with the finding that the glass fiber is not inert.

Previous studies with various mineral particles have suggested that the fibrous geometry of particulates is of critical importance in the generation of superoxide from macrophages (*16,18,35*). For example, for amosite asbestos, dramatic enhancement of release of superoxide has been found with long fibers but not short ones (*35*). The distribution of length of the long fibers (50% > approximately 14 μm long) is similar to that of RF1 (mean length 12.0 μm), and the distribution of length of the short fibers (10% > approximately 10 μm long) is similar to that of MG1 (mean length 3.0 μm). Therefore, our data on the relationship between fiber length and ability to induce CL are consistent with the asbestos data. Moreover, our findings suggest that this relationship continues over the time course without effect of fiber clearance. In contrast, murine peritoneal macrophages exposed to equal numbers of short and long crocidolite asbestos fibers exhibited comparable hydrogen peroxide release (*36*). However, the mean length of the long crocidolite fiber was 5.4 μm, and the mean length of short fiber was 1.2 μm. Our finding that the ability to induce CL was similar among fibers under approximately 6 μm in length was also consistent with the hydrogen peroxide data.

These assays were performed with suspended cells over a time course of 2 hr. Many previous published studies of effects of asbestos and mineral fibers on oxidant production from alveolar macrophages have used cells in suspension. However, many studies of the effect of fiber length on oxidant production and using monocyte-derived macrophages have used adherent cells. For some applications, suspended cells work better than adherent cells for comparing the response of cells. First, the number of cells in each vial will be identical with that of cell suspension. Second, the cells will have diffuse contact with the fibers. We believe that this advantage contributes to linearity of the dose–response curve of CL response. Finally, the cells may smoothly phagocytose the fiber. We consider that these advantages help reduce experimental error.

One problem is whether wollastonite is an exception. Although WO1 was excluded in our analyses, r^2 and β_1 of WO1 increased

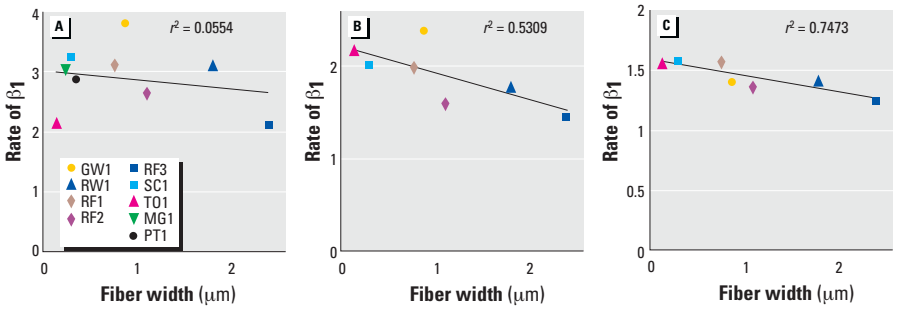

Figure 5. The relationship between geometric-mean width and rate of β_1. The continuous line is a regression line on the whole. (*A*) Data at 15–30 min. (*B*) Data at 30–45 min. (*C*) Data at 45–60 min; this correlation is the highest. The data for $r^2 < 0.9$ were excluded.

Table 6. Constants and the r^2 of the regression lines for the rate of increase in Table 2 and fiber width.

No.[a]	1	2	3	4	5	6	7
A[b]	–0.161	–0.290	–0.139	0.012	–0.029	0.029	0.001
B[b]	3.016	2.213	1.597	1.276	1.101	1.012	1.025
r^{2c}	0.055	0.531	0.747	0.010	0.316	0.505	0.044
n[d]	9	7	7	6	6	4	4

[a]Time-course order of the rate of increase in Table 2. [b]Constants of the regression line for the rate in Table 2 and fiber width. Equation: Y = AX+B; Y = the rate in Table 2, X = geometric-mean width of fibers. [c]Square of the correlation coefficient of the regression line. [d]Effective number. The data < 0.9 in r^2 of Table 1 were excluded.

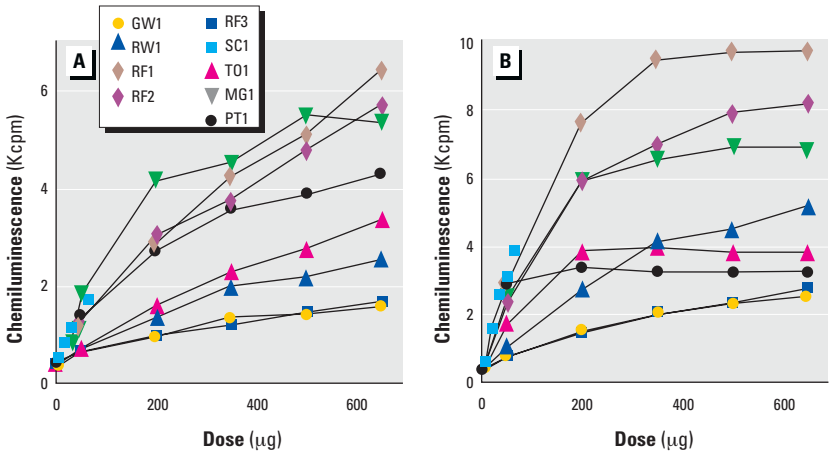

Figure 6. The relationship between sample weight and CL response. (*A*) Data at 45 min. (*B*) Data at 120 min. The data of WO1 were excluded.

Table 7. A slope of regression line of each dose–response curve at 45 min in mass concentration.

Sample	GW1	RW1	MG1	RF1	RF2	RF3	PT1	SC1	TO1
Slope (CL/mg)	1.744	3.264	7.285	8.980	7.777	1.887	5.658	20.18	4.495

Each r^2 was the same as that of Table 1.

over the time course (Table 1). The response for WO1 may be retarded; however, our data are not sufficient to define WO1 as an exception.

In conclusion, it is suggested that macrophages nonspecifically induce superoxide for various fiber types depending on fiber length. Although the generation of hydroxyl radical may be the most important difference between amphibole asbestos and other mineral fibers, superoxide is a tumor promoter and is involved in the generation of hydroxyl radical. Our findings suggested that even inert mineral fibers were not safe if the conditions of durability, clearance, and respirability are satisfied. Our findings have also revealed important differences from the hypothesis that oxidant release occurs during "frustrated" phagocytosis. A remaining problem is to elucidate the reasons why macrophages have high superoxide activity for long fibers.

References and Notes

1. Craighead JE, Mossman BT. The pathogenesis of asbestos-associated diseases. N Engl J Med 306:1446–1455 (1982).
2. Mossman BT, Bignon J, Corn M, Seaton A, Gee JB. Asbestos: scientific developments and implications for public policy. Science 24:294–301 (1990).
3. Ellouk SA, Jaurand MC. Review of animal/*in vitro* data on biological effects of man-made fibers. Environ Health Perspect 102(suppl 2):47–61 (1994).
4. McConnell EE, Wagner JC, Skidmore JW, Moore JA. A comparative study of the fibrogenic and carcinogenic effects of UICC Canadian chrysotile B asbestos and glass microfibre (JM 100). In: Biological Effects of Man-Made Mineral Fibres. Proceedings of a WHO/IARC Coference, Vol 2. Copenhagen:World Health Organization, 1984;234–252.
5. Wagner JC, Berry GB, Hill RJ, Munday DE, Skidmore JW. Animal experiments with MMM(V)F: effects of inhalation and intrapleural inoculation in rats. In: Biological Effects of Man-Made Mineral Fibres. Proceedings of a WHO/IARC Coference, Vol 2. Copenhagen:World Health Organization, 1984;209–233.
6. Bunn WB, Bender JR, Hesterberg TW, Chase GR, Konzen JL. Recent studies of man-made vitreous fibers. J Occup Med 35:101–113 (1993).
7. Hesterberg TW, Chase G, Axten C, Miller WC, Musselman RP, Kamstrup O, Hadley J, Morscheidt C, Bernstein DM, Thevenaz P. Biopersistence of synthetic vitreous fibers and amosite asbestos in the rat lung following inhalation. Toxicol Appl Pharmacol 151:262–275 (1998).
8. Stanton MF, Layard M, Tegeris A, Miller E, May M, Morgan E, Smith A. Relation of particle dimension to carcinogenicity in amphibole asbestoses and other fibrous minerals. J Natl Cancer Inst 67:965–975 (1981).
9. Davis JM, Addison J, Bolton RE, Donaldson K, Jones AD, Smith T. The pathogenicity of long versus short fibre samples of amosite asbestos administered to rats by inhalation and intraperitoneal injection. Br J Exp Pathol 67:415–430 (1986).
10. Roller M, Pott F, Kamino K, Althoff GH, Bellmann B. Results of current intraperitoneal carcinogenicity studies with mineral and vitreous fibres. Exp Toxicol Pathol 48:3–12 (1996).
11. Kamp DW, Graceffa P, Pryor WA, Weitzman SA. The role of free radicals in asbestos-induced diseases. Free Radic Biol Med 12:293–315 (1992).
12. Hardy JA, Aust AE. Iron in asbestos chemistry and carcinogenicity. Chem Rev 95:415–430 (1986).
13. Shull S, Manohar M, Marsh KP, Janssen YM, Mossman BT. Role of iron and reactive oxygen species in asbestos-induced lung injury. In: Free Radical Mechanisms of Tissue Injury (Moslen T, Smith CV, eds). Boca Raton, FL:CRC Press, 1992;153–162.
14. Brown DM, Fisher C, Donaldson K. Free radical activity of synthetic vitreous fibers: iron chelation inhibits hydroxyl radical generation by refractory ceramic fiber. J Toxicol Environ Health 53:545–561 (1998).
15. Pott F, Schlipkoter HW, Ziem U, Spurny K, Huth F. New results from implantation experiments with mineral fibers. In: Biological Effects of Man-Made Mineral Fibres. Proceedings of a WHO/IARC Conference, Vol 2. Copenhagen: World Health Organization, 1984;285–302.
16. Mossman BT, Marsh JP, Shatos MA, Doherty J, Gilbert R, Hill S. Implication of oxygen species as second messengers of asbestos toxicity. Drug Chem Toxicol 10:157–180 (1987).
17. Mossman BT, Sesko AM. *In vitro* assays to predict the pathogenicity of mineral fibers. Toxicology 60:53–61 (1990).
18. Hansen K, Mossman BT. Generation of superoxide from alveolar macrophages exposed to asbestiform and nonfibrous particles. Cancer Res 47:1681–1686 (1987).
19. Ruotsalainen M, Hirvonen MR, Luoto K, Savolainen KM. Production of reactive oxygen species by man-made vitreous fibres in human polymorphonuclear leukocytes. Hum Exp Toxicol 18:354–362 (1999).
20. Ohyama M, Otake T, Morinaga K. The chemiluminescent response from human monocyte-derived macrophages exposed to various mineral fibers of different sizes. Ind Health 38:289–293 (2000).
21. Kohyama N, Tanaka I, Tomita M, Kudo M, Shinohara Y. Preparation and characteristics of standard reference samples of fibrous minerals for biological experiments. Ind Health 35:415–432 (1997).
22. Yamato H, Morimoto Y, Tsuda T, Ohgami A, Kohyama N, Tanaka I. Fiber numbers per unit weight of JFM standard reference samples determined with a scanning electron microscope. Ind Health 36:384–387 (1998).
23. Bøyum A. Isolation of mononuclear cells and granulocytes from human blood. Scand J Clin Lab Invest 21:77–89 (1968).
24. Nyberg P, Klockars M. Measurement of reactive oxygen metabolites produced by human monocyte-derived macrophages exposed to mineral dusts. Int J Exp Path 71:537–544 (1990).
25. WHO. Reference Methods for Measuring Man-Made Mineral fibers (MMMF). Copenhagen:World Health Organization, 1985.
26. Asbestiform Fibers. Nonoccupational Health Risks. Washington, DC:National Academy Press, 1984.
27. Vallyathan V, Mega JF, Shi X, Dalal NS. Enhanced generation of free radicals from phagocytes induced by mineral dusts. Am J Respir Cell Mol Biol 6:404–413 (1992).
28. Weitzman SA, Graceffa P. Asbestos catalyzes hydroxyl and superoxide radical generation from hydrogen peroxide. Arch Biochem Biophys 228:373–376 (1984)
29. Fenton HJH. Oxidation of tartaric acid in the presence of iron. J Chem Soc 106:899–910 (1984)
30. Halliwell B, Gutteridge JMC. Oxygen free radicals and iron in relation to biology and medicine: some problems and concepts. Arch Biochem Biophys 246:501–514 (1986)
31. Halliwell B, Gutteridge JMC. Oxygen toxicity, oxygen radicals, transiton metals and disease. Biochem J 219:1–14 (1984)
32. Stanton MF, Laynard M, Tegeris A, Miller E, May M, Kent E. Carcinogenicity of fibrous glass: pleural response in the rat in relation to fiber dimension. J Natl Cancer Inst 58:587–603 (1977).
33. Archer VE. Carcinogenicity of fibers and films: a theory. Med Hypotheses 5:1257–1260 (1979).
34. Hesterberg TW, Axten C, McConnell EE, Oberdörster G, Everitt J, Miiller WC, Chevalier J, Chase GR, Thevenaz P. Chronic inhalation study of fiber glass and amosite asbestos in hamsters: twelve-month preliminary results. Environ Health Perspect 105(suppl 5):1223–1229 (1997).
35. Hill IM, Beswick PH, Donaldson K. Differential release of superoxide anions by macrophages treated with long and short fibre amosite asbestos is a consequence of differential affinity for opsonin. Occup Environ Med 52:92–96 (1995).
36. Goodglick LA, Kane AB. Cytotoxicity of long and short crocidolite asbestos fibers *in vitro* and *in vivo*. Cancer Res 50:5153–5163 (1990).